Orbital degeneracy and the microscopic model of the FeAs plane in the iron-based superconductors

2008 J. Phys.: Condens. Matter 20 425203

(http://iopscience.iop.org/0953-8984/20/42/425203)

IOP PUBLISHING JOURNAL OF PHYSICS: CONDENSED MATTER

J. Phys.: Condens. Matter **20** (2008) 425203 (6pp) doi:10.1088/0953-8984/20/42/425203

Orbital degeneracy and the microscopic model of the FeAs plane in the iron-based superconductors

Tao Li

Department of Physics, Renmin University of China, Beijing, 100872, People's Republic of China

Received 7 April 2008, in final form 27 July 2008
Published 9 September 2008
Online at stacks.iop.org/JPhysCM/20/425203

Abstract

A microscopic model for the FeAs plane in the newly discovered iron-based superconductors is proposed with the emphasis on the role of the orbital degeneracy between the Fe $3d_{xz}$ and $3d_{yz}$ orbitals in the crystal field environment. The model predicts that the Fe $3d_{xz}$ and $3d_{yz}$ orbitals have the largest itinerancy among the five Fe 3d orbitals as a result of their hybridization with the As 4p orbital. The covalence with the As 4p orbital also explains naturally the large geometric frustration which is necessary for the formation of the magnetic order with a wavevector at $(\pi, 0)$ as found in experiments. An extended s-wave pairing is proposed for the superconducting state based on symmetry considerations and the local magnetic correlation pattern.

(Some figures in this article are in colour only in the electronic version)

The newly discovered iron-based superconductors, F-doped LaOFeAs [1] and its derivatives [2–5] with rare earth substitution, have given rise to much interest in the research community. Similar to the high-T_c cuprates, the iron-based superconductors also have a layered structure in which the role of the copper–oxygen plane in the high-T_c cuprates is played by the FeAs plane. In both systems, the charge dopant and the doped carrier are separated spatially, which produces an ideal environment for the coherent motion of the latter at an incommensurate band filling. This similarity may imply that a still higher T_c is possible in this series of compounds by optimizing the interlayer distance and planeness of the FeAs layer.

Band structure, as calculated from density functional theory (DFT) and its DMFT improvement, has been examined by several groups [6–10]. Not surprisingly, most of the spectral weight close to the Fermi energy is contributed by the Fe 3d orbital, as the Fe is the only ion in the system that possesses an unclosed shell. The DFT calculation also predicts an antiferromagnetic ordered ground state for the parent compound LaOFeAs with an ordering wavevector at $(\pi, 0)$, which is confirmed by neutron scattering experiments [11].

Based on the results of the DFT calculations, several phenomenological theories for the doped iron-based superconductors have been proposed [12–14]. In this paper, we follow instead the quantum chemistry considerations and propose a tight binding microscopic model for the FeAs plane. In our model, the orbital degeneracy between the Fe $3d_{xz}$ and $3d_{yz}$ orbital plays an essential role. The model predicts that the Fe $3d_{xz}$ and $3d_{yz}$ orbital have the largest itinerancy among the five Fe 3d orbitals as a result of their hybridization with the As 4p orbital. The covalence with the As 4p orbital also explains naturally the large geometric frustration which is necessary for the formation of the magnetic order with a wavevector at $(\pi, 0)$, as found in experiments. Based on symmetry considerations and the local magnetic correlation pattern, we propose an extended s-wave pairing for the superconducting state.

A key issue for the construction of a microscopic model for the FeAs plane is to elucidate the role of the orbital degeneracy of the five Fe 3d orbitals. In the presence of crystal field, the five-fold degenerate Fe 3d atomic orbital will split according to the irreducible representations of the crystal symmetry and not all five 3d orbitals are equally important for the low energy physics. According to the DFT calculation, the crystal splitting of the Fe 3d orbital is small and all five Fe 3d orbitals should be included in the model in principle. However, the inclusion of the electron correlation effect can enhance the crystal splitting and vice versa. At the same time, the five Fe 3d orbitals have quite different hopping integrals as a result

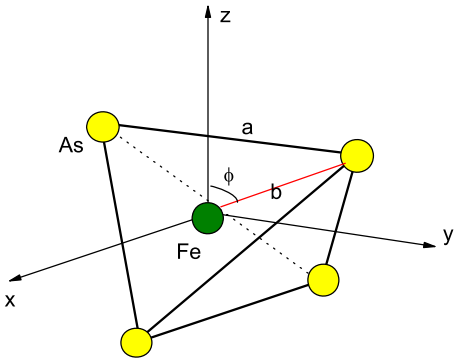

Figure 1. The squashed tetrahedron formed by four neighboring As ion around each Fe ion in the FeAs plane. From the lattice constant reported in the literature, $a = 4.020$ Å, $b = 2.35$ Å, the angle ϕ between the Fe–As bond with the normal of the Fe–As plane is estimated to be 58.8°, while in a perfect tetrahedron the angle would be 54.7°. Here we use a coordinate system in which the x and y axes point along the As–As bond directions.

of their different hybridization with the As 4p orbital. Here we assume the crystal field splitting and the orbital selective hopping effect to be sufficiently strong to retain only the Fe $3d_{xz}$ and $3d_{yz}$ for the discussion of the low energy physics.

In the FeAs plane, each Fe ion sits at the center of inversion of a squashed (along the normal of the FeAs plane) tetrahedron formed by four neighboring As ions (see figure 1). Using the lattice constants reported in the literature [7], one estimates that the Fe–As bond makes an angle of about 58.8° with the normal of the FeAs plane, while in a perfect tetrahedron the corresponding angle should be 54.7°. In an ideal tetrahedron environment, the five-fold degenerate Fe 3d orbital will split into the E_g doublet ($3d_{3z^2-r^2}$ and $3d_{xy}$) and the t_{2g} triplet ($3d_{xz}$, $3d_{yz}$, and $3d_{x^2-y^2}$). If we assume that the crystal field is contributed mainly by the four neighboring As ions, one would expect the two E_g orbitals to have lower energy than the three t_{2g} orbitals, as the electron cloud of the E_g orbital points towards the vacancy of the As ion while the electron cloud of the t_{2g} orbital points towards the As ion (see figure 2). When the tetrahedron is squashed along the z direction, the degeneracy between the $3d_{3z^2-r^2}$ orbital and the $3d_{xy}$ orbital will be lifted and the $3d_{3z^2-r^2}$ orbital will have a lower energy than that of the $3d_{xy}$ orbital, as the electron cloud of the $3d_{3z^2-r^2}$ orbital has a better chance of avoiding the As ion (see figure 2). Similarly, the degeneracy between the $3d_{xz}$ ($3d_{yz}$) orbital and the $3d_{x^2-y^2}$ orbital will be lifted and the $3d_{x^2-y^2}$ orbital will have a higher energy than that of the $3d_{xz}$ and $3d_{yz}$ orbitals. In the tetragonal structure of the FeAs plane, the degeneracy between the $3d_{xz}$ and $3d_{yz}$ orbitals is protected by symmetry.

The divalent Fe ions in the FeAs plane have six electrons in their 3d shell. According to the above splitting scheme, one would expect a very peculiar situation to occur in the parent compounds in which the Fermi energy lies within two degenerate bands which are both half-filled. We think this is the reason why the parent compounds, with six electrons in five 3d orbitals, are neither usual band insulators nor a usual band metals. It may also hold the key to explain why the lightly doped LnOFeAs system shows such remarkable properties as having a T_c as high as 50 K [5].

In the following, we assume the crystal splitting to be large enough to neglect the filled $3d_{3z^2-r^2}$ and $3d_{xy}$ band and the empty $3d_{x^2-y^2}$ band in the discussion of low energy physics. With this simplification, we are left with a model with two degenerate bands. In this model, each Fe site can accommodate at most four electrons in the two degenerate bands. In the parent compound, each Fe site has two electrons on average in the two degenerate bands and the system is thus half-filled.

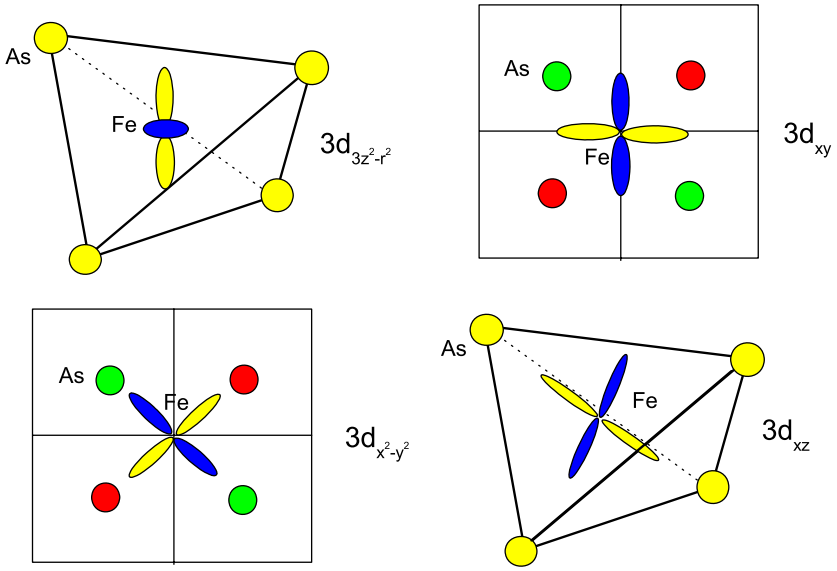

Figure 2. The five d orbitals in the crystal field of the tetrahedron formed by the four neighboring As ions around each Fe ion. The $3d_{x^2-y^2}$ and the $3d_{xy}$ orbitals are shown here in a projection onto the xy plane. In the projection graph, red/light gray (green/dark gray) filled circles denote As ion above (below) the xy plane. Here we only show the $3d_{xz}$ orbital, the $3d_{yz}$ orbital can be obtained from the $3d_{xz}$ orbital through a rotation of $\frac{\pi}{2}$ along the z-axis.

The interactions between the electrons on the same Fe site can be classified into three types, namely the intra-orbital Hubbard repulsion U, the spin independent part of the inter-orbital Hubbard repulsion U_1, and the spin dependent part of the inter-orbital Hubbard repulsion J (the usual Hund's rule coupling). From the definition of these terms, one easily sees that the inequality $U > U_1 > \frac{J}{4} > 0$ should be satisfied. These interaction terms are represented by the model Hamiltonian

$$\begin{aligned} H_U = & U \sum_i (n_{i,xz,\uparrow} n_{i,xz,\downarrow} + n_{i,yz,\uparrow} n_{i,yz,\downarrow}) \\ & + U_1 \sum_i (n_{i,xz,\uparrow} + n_{i,xz,\downarrow})(n_{i,yz,\uparrow} + n_{i,yz,\downarrow}) \\ & - J \sum_i \vec{S}_{i,xz} \cdot \vec{S}_{i,yz} \end{aligned} \tag{1}$$

in which $n_{i,xz,\uparrow} = c^{\dagger}_{i,xz,\uparrow} c_{i,xz,\uparrow}$ denotes the number of up spin electrons in the $3d_{xz}$ orbital. $\vec{S}_{i,xz} = \frac{1}{2} c^{\dagger}_{i,xz,\alpha} \vec{\sigma}_{\alpha,\beta} c_{i,xz,\beta}$ denotes the spin density on the $3d_{xz}$ orbital. The meaning of other terms in the equation is similar.

We now consider the kinetic energy of the Fe 3d electrons. The Fe 3d electrons can hop between Fe sites either directly or through the indirect hopping process bridged by the As 4p orbital (see figure 3). Since the As ions sit above (or below) the center of the Fe plaquette, the As bridged hopping is much more effective for the $3d_{xz}$ and $3d_{yz}$ orbitals than for other Fe 3d orbitals, as their electron clouds have the best chance to reach the As ion. Such an orbital selective hopping effect provides a natural explanation for the much larger itinerancy of the $3d_{xz}$ and $3d_{yz}$ bands as compared to other 3d bands found in DFT calculations [7]. In the following, we will assume that the As bridged hopping is the main contribution to the kinetic energy of the $3d_{xz}$ and $3d_{yz}$ bands and neglect the direct hopping for these two bands for simplicity (the itinerancy of other Fe 3d bands still comes from direct hopping).

The As ion has three 4p orbitals in its outmost shell. Since the $4p_z$ orbital is far away from the Fermi energy, we consider only the hopping path mediated by the $4p_x$ and $4p_y$ orbitals of the As ion. As a result of the sign change between the two lobes of the $3d_{xz}$ orbital, an electron in the $3d_{xz}$ orbital can hop only via the As $4p_x$ orbital. Similarly, an electron in the $3d_{yz}$ orbital can hop only via the As $4p_y$ orbital. Thus, the indirect hopping mediated by the As $4p_x$ and $4p_y$ orbitals conserves the orbital index, namely, an electron initially on the Fe $3d_{xz}(3d_{yz})$ orbital can only hop onto the $3d_{xz}(3d_{yz})$ orbital of the destination Fe ion (the inclusion of the hopping path mediated by the $4p_z$ orbital will break such a symmetry) (see figure 3).

Another peculiarity about the As ion aided effective hopping is that the hopping integral between next-nearest-neighboring Fe ions is anisotropic (the hopping between nearest neighboring Fe ions remains isotropic) and thus breaks the tetragonal symmetry down to orthogonal. This anisotropy originates from the anisotropic nature of the $3d_{xz}$ and $3d_{yz}$ orbital. To be more specific, we introduce two kinds of hopping integral, t_A and t_B, to denote the σ-like and π-like hybridization between the $3d_{xz}(3d_{yz})$ orbital and the corresponding $4p_x(4p_y)$ orbital shown in figure 3. Then, the

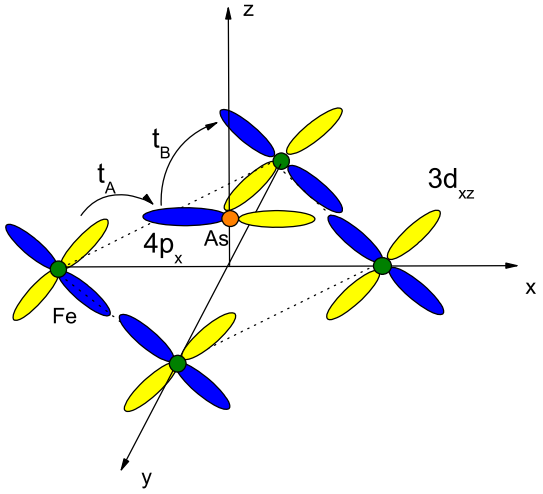

Figure 3. A schematic representation of the As 4p orbital aided hopping between neighboring Fe ions on the square lattice. Note that the As ions lie above or below the Fe plane. Simple symmetry considerations show that the electron on the Fe $3d_{xz}(3d_{yz})$ orbital can hop only through the As $4p_x(4p_y)$ orbital. This explains the conservation of the orbital index and the anisotropy of the hopping Hamiltonian. The electron wavefunction on the yellow/light gray (blue/dark gray) lobes have positive (negative) values. t_A denotes the σ-like hybridization between the $3d_{xz}(3d_{yz})$ and the $4p_x(4p_y)$ orbital, t_B denotes the π-like hybridization between the $3d_{xz}(3d_{yz})$ and the $4p_x(4p_y)$ orbital.

As bridged hopping terms between neighboring Fe sites are given approximately by

$$t = 2\frac{t_A t_B}{\Delta}, \qquad t_1 = \frac{t_A^2}{\Delta}, \qquad t_2 = \frac{t_B^2}{\Delta}, \tag{2}$$

in which t denotes the hopping integral between nearest neighboring (NN) Fe sites, t_1 and t_2 denote the hopping integrals between next nearest neighboring (NNN) Fe sites in the two diagonal directions, Δ denotes the energy splitting between the Fe $3d_{xz}(3d_{yz})$ orbital and the As $4p_x(4p_y)$ orbital. The factor of two for t comes from the fact that there are two hopping paths between the nearest neighboring Fe ions.

Taking all these considerations into account, we arrive at the following model for the effective hopping between the Fe ions.

$$\begin{aligned} H_t = & -t \sum_{i,\vec{\delta},\sigma} \left[(c^{\dagger}_{i,xz,\sigma} c_{i+\vec{\delta},xz,\sigma} + c^{\dagger}_{i,yz,\sigma} c_{i+\vec{\delta},yz,\sigma}) + \text{H.C.} \right] \\ & - t_1 \sum_{i,\sigma} \left[(c^{\dagger}_{i,xz,\sigma} c_{i+\vec{\delta}',xz,\sigma} + c^{\dagger}_{i,yz,\sigma} c_{i+\vec{\delta}'',yz,\sigma}) + \text{H.C.} \right] \\ & - t_2 \sum_{i,\sigma} \left[(c^{\dagger}_{i,xz,\sigma} c_{i+\vec{\delta}'',xz,\sigma} + c^{\dagger}_{i,yz,\sigma} c_{i+\vec{\delta}',yz,\sigma}) + \text{H.C.} \right], \end{aligned} \tag{3}$$

in which $\vec{\delta} = \vec{e}_x$ or $\vec{e}_x$ denote the nearest neighboring vectors on the square lattice formed by Fe ions. $\vec{\delta}' = \vec{e}_x + \vec{e}_y$ and $\vec{\delta}'' = \vec{e}_x - \vec{e}_y$ denotes the next nearest neighboring vectors. From figure 3, it is easy to see that t_A and t_B have different signs. As a result, $t < 0$ and $t_1, t_2 > 0$. However, on the square lattice, the sign of nearest neighboring hopping can be

made positive with a suitable choice of gauge. In the below, we will take $t > 0$.

The dispersion relation of the $3d_{xz}$ and the $3d_{xz}$ band are given by

$$\begin{aligned}\varepsilon_{xz,k} &= -2t(\cos(k_x) + \cos(k_x)) - 2t_1\cos(k_x + k_y) \\ &\quad - 2t_2\cos(k_x - k_y) \\ \varepsilon_{yz,k} &= -2t(\cos(k_x) + \cos(k_x)) - 2t_2\cos(k_x + k_y) \\ &\quad - 2t_1\cos(k_x - k_y).\end{aligned} \tag{4}$$

Thus, although the dispersion relation of the $3d_{xz}$ and the $3d_{xz}$ band individually break the tetragonal symmetry, the system as a whole still possesses tetragonal symmetry.

The total Hamiltonian of the system is the sum of the on-site term H_U and the hopping term H_t. Before looking at the phase diagram of the model, we first estimate the model parameters. According to DFT calculations, the Hubbard repulsions U and U_1 are about 4 eV in magnitude and the Hund's rule coupling J is about 1 eV in magnitude. For the hopping terms, as both the Fe $3d_{xz}$–As $4p_x$ separation and the hopping integral between the two are of the order of 1 eV, we estimate the effective hopping integral between the Fe ions mediated by the As ions to be also of the order of 1 eV. Thus the system has a moderate level of electron correlation. Another important interaction parameter is the ratio between the NNN and NN hopping integral. In our model, the ratio is given by

$$\frac{t_1}{t} = \frac{1}{2}\frac{t_A}{t_B}, \qquad \frac{t_2}{t} = \frac{1}{2}\frac{t_B}{t_A}. \tag{5}$$

Thus, the NNN to NN hopping ratio is at least 0.5, much larger than one would expect if there were only direct hopping.

Now we discuss the possible phase diagram of the model. In the half-filled parent compounds, each site is occupied on average by two electrons. Since the intra-orbital Hubbard repulsion U is larger than the inter-orbital Hubbard repulsion U_1, the two electrons tend to occupy different orbitals and the remaining Hund's rule coupling tends to align the spin of the electrons on both orbitals. Thus each individual Fe ion carries approximately a unit spin angular momentum and shows two Bohr magnetons of magnetic moment.

The inclusion of the hopping terms between the Fe ions will induce antiferromagnetic spin exchange between neighboring Fe ions within each band. Since the frustration ratio is already quite large, it is a nontrivial problem as to what kind of magnetic order is favored for the realistic model parameter. To elucidate this problem, we conduct a mean field calculation on the magnetic order for the half-filled system. For simplicity, we restrict our calculation to colinear magnetic order with the ordering wavevector at (π, π) and $(\pi, 0)$. The mean field Hamiltonian, apart from the chemical potential term and the constant energy term, is given by

$$\mathrm{H_{MF}} = H_t - (2U + J)\sum_i M_i(S^z_{i,xz} + S^z_{i,yz}), \tag{6}$$

in which $M_i = \frac{1}{2}\langle\sum\sigma n_{i,xz,\sigma}\rangle = \frac{1}{2}\langle\sum\sigma n_{i,yz,\sigma}\rangle = M\exp(\mathrm{i}\vec{Q}\cdot\vec{R}_i)$ is the order parameter for the magnetic order, $\vec{Q} = (\pi, \pi)$ or $(\pi, 0)$ is the ordering wavevector. From the mean field Hamiltonian, we find that the Hund's coupling acts to enhance the effect of the intra-orbital Hubbard U term and in the following we take it into account by defining $\widetilde{U} = U + \frac{J}{2}$.

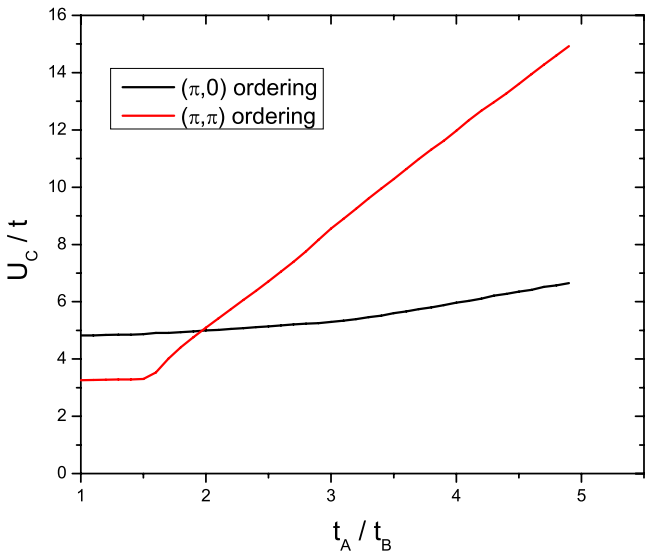

Figure 4. The critical value for the formation of magnetic order at (π, π) and $(\pi, 0)$ as a function of the frustration ratio $\frac{t_A}{t_B}$.

The mean field self-consistent equation for the order parameter is given by

$$1 = \frac{2\widetilde{U}}{N}\sum_k\left[\frac{(\xi_k - E^+_k)n^+_k}{\Delta^2_{\mathrm{AF}} + (\xi_k - E^+_k)^2} + \frac{(\xi_k - E^-_k)n^-_k}{\Delta^2_{\mathrm{AF}} + (\xi_k - E^-_k)^2}\right], \tag{7}$$

in which the sum is over the reduced Brillouin zone of the corresponding magnetic order, $n^\pm_k = 1 - \theta(E^\pm_k)$, $\Delta_{\mathrm{AF}} = \widetilde{U}M$. $E^\pm_k$ is given by

$$E^\pm_k = \frac{\xi_k + \xi_{k+\vec{Q}} \pm \sqrt{(\xi_k - \xi_{k+\vec{Q}})^2 + 4\Delta^2_{\mathrm{AF}}}}{2}, \tag{8}$$

in which $\xi_k = \varepsilon_{xz,k} - \mu$ and the chemical potential μ is determined by the half-filling condition.

We have solved the self-consistent equation numerically. Figure 4 shows the critical value $\widetilde{U}_c$ for the formation of magnetic order at wavevector (π, π) and $(\pi, 0)$ as a function of $\frac{t_A}{t_B}$. We find that the critical value for both orders increases with the frustration ratio $\frac{t_A}{t_B}$ and the order with a lower critical value is always more stable. Thus, for $\frac{t_A}{t_B} < 2$, or $\frac{t_1}{t} < 1$, the (π, π) order is more stable, while for $\frac{t_A}{t_B} > 2$, or $\frac{t_1}{t} > 1$, the $(\pi, 0)$ order becomes more stable. The $(\pi, 0)$ order observed in experiment then indicates that the system is strongly frustrated. The As ion bridged indirect hopping proposed in our model seems to be the only way to account for such strong geometrical frustration.

Figure 5 shows the ordered moment calculated at a fixed frustration ratio $\frac{t_A}{t_B} = 2.5$ for $\vec{Q} = (\pi, 0)$. We find that the ordered moment increases abruptly from zero to a value of order $2\mu_{\mathrm{B}}$ above the critical interaction value. Such a first order transition behavior is caused by geometrical frustration. Experimental detection of such a transition can be interesting.

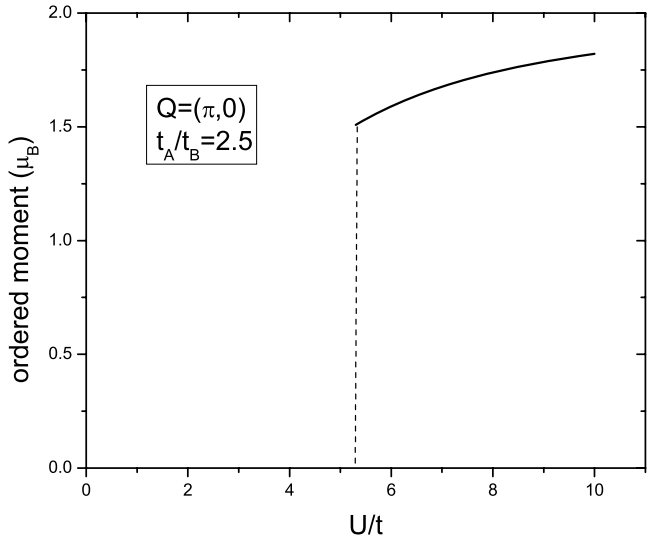

Figure 5. The ordered magnetic moment as a function of $\frac{\tilde{U}}{t}$ with the frustration ratio fixed at $\frac{t_A}{t_B} = 2.5$ and $\vec{Q} = (\pi, 0)$.

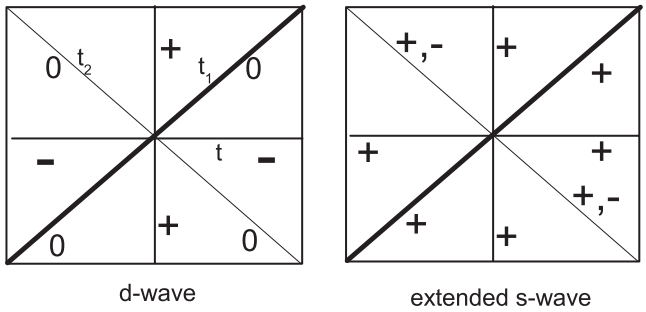

Figure 6. The sign structure of the d-wave and extended s-wave pairing amplitudes in real space. Bonds in the different thicknesses have different strengths of the hopping integral. In the extended s-wave case, the pairing amplitude on NN bonds can be made positive with gauge transformation.

Finally we discuss the superconducting phase at finite doping. As in the cuprate superconductors, the antiferromagnetic superexchange responsible for the magnetic ordering at half-filling will also induce electron pairing at finite doping in the singlet channel. A quantitative analysis of such pairing instability in our model is beyond the scope of the present work. Here we present a qualitative analysis of the possible pairing symmetry in the singlet channel.

In our model, the antiferromagnetic superexchange takes place within each band and thus the singlet pairing induced by it is an intra-band electron pairing. As we have mentioned above, the $3d_{xz}$ and the $3d_{yz}$ band individually each have an orthogonal symmetry (see figure 6). Thus we should classify the intra-band electron pairing according to the orthogonal rather than the tetragonal point group. For the orthogonal point group C_{2v}, there are two irreducible representations in the singlet channel, namely the d-wave pairing and the extended s-wave pairing representation. The sign structure for both pairing symmetries in real space is illustrated in figure 6. In the d-wave pairing case, the pairing amplitudes are odd with respect to the reflection in the two diagonal directions and thus the pairing amplitudes in these two directions are forced to be zero. In the extended s-wave pairing case, the pairing amplitude is even with respect to both reflections and thus can be nonzero in all directions.

As we have mentioned above, the $(\pi, 0)$ magnetic order at half-filling is stable only when $t_1 > t$. In such a case, the superexchange in the diagonal direction with hopping integral t_1 should be the strongest and we would expect the strongest singlet pairing in this direction. This is obviously inconsistent with the d-wave paring symmetry which enforces the pairing amplitude in the diagonal direction to be zero. Thus we believe the extended s-wave pairing is the most possible pairing symmetry, provided that the magnetic exchange is the origin of the pairing.

The above argument can also be formulated in the momentum space as follows. According to the weak coupling analysis, the pairing gap induced by the exchange of magnetic fluctuation peaked at momentum $\vec{Q}$ should satisfy the following inequality on the Fermi surface [16]

$$\Delta_k \Delta_{k+\vec{Q}} < 0. \tag{9}$$

For $\vec{Q} = (\pi, 0)$, this inequality is incompatible with the d-wave pairing which has a gap function of the form $\cos(k_x) - \cos(k_y)$, but can be compatible with the extended s-wave pairing if the pairing amplitudes along the diagonal direction are large enough.

Up to now, we have neglected the inter-orbital couplings in our discussion of the superconductivity. In the presence of such couplings, the Cooper pairs in the two bands get entangled with each other. Such entanglement will inevitably increase the effective mass of the Cooper pair in each band and reduce the superfluid density. More specifically, the Hund's rule coupling will induce entanglement between the Cooper pairs in the spin channel (in a way much like the projection operator does in the construction of the matrix-product-type ground state for the Affleck–Kennedy–Lieb–Tasaki (AKLT) model [15]), while the inter-orbital Hubbard interaction will induce entanglement in the charge channel. Since the Hund's rule coupling tends to enlarge the spin value at each site and thus enhance the classical nature of the electron spin, it seems to be at odds with the spin singlet pairing which is of totally quantum nature. Thus, in addition to the entanglement effect, the Hund's rule coupling seems to also suppress electron pairing in the singlet channel. A detailed analysis of these interesting problems is left for future works.

In summary, a microscopic model for the FeAs plane of the newly discovered iron-based superconductors is proposed. In our model, the orbital degeneracy between the Fe $3d_{xz}$ and $3d_{yz}$ orbitals plays an essential role. The model predicts that the Fe $3d_{xz}$ and $3d_{yz}$ orbitals have the largest itinerancy among the five Fe 3d orbitals as a result of their hybridization with the As 4p orbital. The covalence with the As 4p orbital also explains naturally the large geometric frustration which is necessary for the formation of the magnetic order with a wavevector at $(\pi, 0)$. Based on symmetry considerations and the local magnetic correlation pattern, we propose an extended s-wave pairing for the superconducting state.

Acknowledgments

This work is supported by NSFC grant No. 10774187. The author acknowledges the discussion with Professors Zheng-Yu Weng, Ya-Yu Wang, Yue-Hua Su, and Kai Wu.

References

[1] Kamihara Y, Watanabe T, Hirano M and Hosono H 2008 *J. Am. Chem. Soc.* **130** 3296
[2] Chen G F, Li Z, Li G, Zhou J, Wu D, Dong J, Hu W Z, Zheng P, Chen Z J, Luo J L and Wang N L 2008 arXiv:0803.0128 [cond-mat]
[3] Wen H-H, Mu G, Fang L, Yang H and Zhu X 2008 *Europhys. Lett.* **82** 17009
Wen H-H, Mu G, Fang L, Yang H and Zhu X 2008 arXiv:0803.3021 [cond-mat]
[4] Chen X H, Wu T, Wu G, Liu R H, Chen H and Fang D F 2008 *Nature* **453** 761
[5] Ren Z-A, Yang J, Lu W, Yi W, Shen X-L, Li Z-C, Che G-C, Dong X-L, Sun L-L, Zhou F and Zhao Z-X 2008 arXiv:0803.4283 [cond-mat]
[6] Singh D J and Du M-H 2008 arXiv:0803.0429 [cond-mat]
[7] Haule K, Shim J H and Kotliar G 2008 arXiv:0803.1279 [cond-mat]
[8] Xu G, Ming W, Yao Y, Dai X, Zhang S-C and Fang Z 2008 arXiv:0803.1282 [cond-mat]
[9] Cao C, Hirschfeld P J and Cheng H-P 2008 arXiv:0803.3236 [cond-mat]
[10] Ma F and Lu Z-Y 2008 arXiv:0803.3286 [cond-mat]
[11] Cruz C, Huang Q, Lynn J W, Li Jiying, Ratcliff W, Zarestky J L, Mook H A, Chen G F, Luo J L, Wang N L and Dai P 2008 *Nature* **453** 899
[12] Kuroki K, Onari S, Arita R, Usui H, Tanaka Y, Kontani H and Aoki H 2008 arXiv:0803.3325 [cond-mat]
[13] Dai X, Fang Z, Zhou Y and Zhang F-C 2008 arXiv:0803.3982 [cond-mat]
[14] Han Q, Chen Y and Wang Z D 2008 arXiv:0803.4346 [cond-mat]
[15] Affleck I K, Kennedy T, Lieb E H and Tasaki H 1988 *Commun. Math. Phys.* **115** 477
[16] Kampf A P 1994 *Phys. Rep.* **249** 219